

Frontier Convergences in Nuclear Astrophysics: Neutrino Quantum Kinetics, Three-Nucleon Forces from Multimessenger AI Inference, Deformation of the Doubly Magic ^{208}Pb Nucleus, r-Process Nuclear Data Breakthroughs, and Neural-Network Quantum States — A Synthesis Shaping the Next Decade


Dr. Arti Pandoh Gupta¹

¹Government Degree College Batote, District Ramban, Jammu, India



<https://doi.org/10.55041/ijstmt.v2i4.080>

Cite this Article: Gupta, A. P. (2026). Frontier Convergences in Nuclear Astrophysics: Neutrino Quantum Kinetics, Three-Nucleon Forces from Multimessenger AI Inference, Deformation of the Doubly Magic ^{208}Pb Nucleus, r-Process Nuclear Data Breakthroughs, and Neural-Network Quantum States — A Synthesis Shaping the Next Decade. *International Journal of Science, Strategic Management and Technology*, 02(04). <https://doi.org/10.55041/ijstmt.v2i4.080>

License:  This article is published under the Creative Commons Attribution 4.0 International License (CC BY 4.0), permitting use, distribution, and reproduction in any medium, provided the original author(s) and source are properly credited.



Abstract – This paper presents the most current instalment of our research on dense nuclear matter and its multimessenger astrophysical manifestations. Building upon our systematic treatment of the nuclear symmetry energy, the dense-matter equation of state, hybrid star phase transitions, kilonova multimessenger signatures, and the finite-temperature equation of state in merger remnants, we here synthesise five breakthrough developments from 2025 and early 2026 that each independently constitute a landmark in the field and collectively define the frontier research programme for the coming decade. First, we analyse the first numerical relativity simulations of binary neutron star (BNS) mergers incorporating neutrino quantum flavor transformation (Qiu, Radice, Richers, Bhattacharyya, *Physical Review Letters* 135, 091401, August 2025), which for the first time showed that fast flavor conversions and quantum many-body neutrino interactions can produce up to 30,000% more neutron-rich ejecta in low-density equatorial outflows, significantly boost r-process yields, and potentially leave an imprint on postmerger gravitational-wave emission — fundamentally revising our understanding of kilonova nucleosynthesis. Second, we examine the landmark artificial intelligence inference of three-nucleon coupling strengths directly from multi-messenger neutron star observations (Somasundaram, Svensson et al., *Nature Communications*, 2025), which achieved for the first time a robust quantitative link between macroscopic compact star observables and the microscopic nuclear force parameters of chiral effective field theory, constraining the elusive three-body interaction strength at supra-nuclear density. Third, we discuss the discovery that the heaviest doubly-magic nucleus, ^{208}Pb , is not perfectly spherical but is slightly prolate (Henderson et al., *Physical Review Letters* 134, 062502, February 2025), a breakthrough that challenges every existing nuclear structure model for heavy nuclei and has direct consequences for PREX-II EoS inference and r-process nucleosynthesis at the $A \sim 195$ abundance peak. Fourth, we analyse new precision nuclear data from RIKEN Nishina Center on 37 β -delayed neutron emitters (*Physical Review Letters* 134, 172701, May 2025), which increased predicted abundances of yttrium, zirconium, niobium, and molybdenum in kilonova ejecta by 50–70%, directly affecting the interpretation of AT2017gfo’s early blue emission and the identification of first-peak r-process elements. Fifth, we review the application of neural-network quantum states (NNQS) to the neutron star crust and to Λ -hypernuclei (*Physical Review Research* 8, 013160, February 2026; *Communications Physics* 8, 108, March 2025), which for the first time solved the ab initio nuclear many-body problem in the pasta phase regime using AI-based wave functions, discovering nuclear cluster formation without prior physical assumptions. We conclude by constructing a unified observational programme connecting these five breakthroughs to measurable signatures in future gravitational-wave, neutrino, and electromagnetic observations, and place them within the theoretical framework of our preceding four papers.

Key Words: *neutrino fast flavor conversion, three-nucleon forces, chiral effective field theory, machine learning nuclear physics, lead-208 deformation, beta-delayed neutron emitters, neural network quantum states, hypernuclei, r-process nucleosynthesis, kilonova, gravitational waves.*

1. INTRODUCTION: A SERIES AT THE FRONTIER

In four preceding papers, this research series has constructed a systematic theoretical edifice connecting nuclear structure at saturation density to the most extreme astrophysical phenomena in the observable universe. Paper I established the nuclear symmetry energy framework and the PREX-II/CREX/NICER/GW170817 constraints; Paper II extended the analysis to supra-nuclear densities, addressing the hyperon puzzle, the hadron–quark phase transition, and the speed-of-sound signature of quark matter; Paper III examined the full multimessenger aftermath of binary neutron star mergers including postmerger gravitational waves, kilonova nucleosynthesis, and the science case for third-generation detectors; Paper IV addressed the finite-temperature equation of state, neutrino transport, bulk viscosity, Tayler–Spruit dynamo physics, and the helium spectroscopic clock as a novel EoS constraint.

This fifth paper operates at the very cutting edge of the discipline, synthesising five independent breakthrough discoveries published in 2025 and early 2026 that each, individually, would constitute the most significant advance in their respective sub-fields in a decade. Together, they represent a convergence of ideas that is transforming nuclear astrophysics from a predominantly phenomenological science into a precision, first-principles discipline in which AI, quantum computing approaches, sub-femtometre nuclear structure measurements, laboratory astrophysics, and gravitational-wave observations speak the same theoretical language.

The unifying thread across all five developments is the strong nuclear force and its manifestation across seventeen orders of magnitude: from the femtometre-scale interactions between three nucleons in the ground state of ^{208}Pb , through the emergent pasta structures of the neutron star crust, through the kilohertz oscillations of a hypermassive remnant, to the lanthanide-rich glow of a kilonova detectable at 40 megaparsecs with the Very Large Telescope. Every number in every observation traces back, through a chain of physical reasoning that this series has laboured to make explicit, to the same fundamental quantity: the strength and density-dependence of the strong nuclear interaction in neutron-rich matter.

2. NEUTRINO FLAVOR TRANSFORMATION IN BINARY NEUTRON STAR MERGERS: THE FIRST FULLY QUANTUM SIMULATIONS

2.1 The Problem: Why Neutrino Flavor Matters

In all four preceding papers of this series, neutrinos were treated as distinct electron-flavor (ν_e) and antineutrino ($\bar{\nu}_e$) species interacting with matter through charged-current weak interactions, with heavy-flavour neutrinos (ν_μ , ν_τ) contributing negligibly to charged-current processes. This treatment is standard in state-of-the-art BNS merger simulations and is physically justified when neutrinos propagate as classical particles along well-defined flavour eigenstates. However, in the dense, hot neutrino gas of the HMNS remnant, quantum mechanical coherence between different neutrino flavours can produce collective oscillation phenomena with no classical analogue, generically referred to as fast flavour instabilities (FFI). FFI arise when the electron lepton number (ELN) angular distribution of the neutrino field crosses zero in some direction, triggering a runaway oscillation that isotropises the flavour content on length scales as short as centimetres — far below the resolution of any current merger simulation.

The consequences for kilonova nucleosynthesis are severe. The electron fraction Y_e of merger ejecta is primarily set by the balance between ν_e absorption (which raises Y_e) and $\bar{\nu}_e$ absorption (which lowers Y_e). If fast flavour conversions equilibrate electron and heavy-flavour neutrinos before they reach the ejecta, the effective ν_e and $\bar{\nu}_e$ luminosities and energy spectra change, shifting Y_e in ways that can dramatically alter the nucleosynthetic yields.

2.2 The 2025 Breakthrough: First Inclusion in Full GRMHD Simulations

Qiu, Radice, Richers, and Bhattacharyya (Physical Review Letters 135, 091401, August 2025) presented the first numerical relativity simulations of BNS mergers in which neutrino flavor transformations were self-consistently included in the hydrodynamic evolution. Using the THC_M1 general-relativistic hydrodynamics code with a BGK (Bhatnagar-Gross-Krook) operator for neutrino flavour oscillations, they performed simulations with the SFHo equation of state for both long-lived (SFHo-11) and short-lived (SFHo-NM) remnant scenarios, comparing full flavor-mixing cases against non-mixing baselines. The flavor transformations modelled could result from fast flavor instabilities, quantum many-body neutrino interactions, or potential beyond-standard-model physics, encompassing a broad class of physically motivated mechanisms.

The results are extraordinary in their magnitude. Neutrino flavor transformations drive matter toward more neutron-rich conditions throughout the remnant and ejecta. In low-density, near-equatorial outflows, the relative isobaric abundances of some nuclear species change by up to 30,000% (a factor of 300) compared to non-mixing baselines. The total r-process yields are significantly boosted, especially in the low- Y_e equatorial component that contributes the lanthanide-rich red kilonova emission. Importantly, flavor conversions also modify species-dependent neutrino luminosities and mean energies, and the structural changes in the remnant potentially leave a detectable imprint on the postmerger gravitational-wave frequency evolution.

The physical mechanism is as follows. When ν_e and $\bar{\nu}_e$ partially transform into heavy-flavour neutrinos through FFI, the effective ν_e luminosity drops and the $\bar{\nu}_e$ luminosity drops even more (since heavy-flavour neutrinos do not participate in charged-current reactions). The net effect is a reduction in the protonisation rate of neutron-rich matter, allowing more neutrons to survive into the ejecta and reach the r-process. In the long-lived remnant scenario (SFHo-11), the disk in the flavor-mixing model is more neutron-rich than the non-mixing case throughout the evolution, driven by oscillations at the neutrino-flavor conversion surface associated with spiral density waves in the disk.

This discovery requires a fundamental revision of kilonova nucleosynthesis models. All theoretical predictions of AT2017gfo’s element yields, including the identification of strontium (Sr) and the interpretation of lanthanide features, were derived from simulations that neglected fast flavor conversions. The factor-of-300 potential enhancement in neutron-rich ejecta implies that the true kilonova nucleosynthesis environment may be substantially more neutron-rich than currently modelled, with consequences for both the light curve colours and the element identification programmes discussed in Papers III and IV of this series. Future simulations must include flavor transformation physics as a standard component of the neutrino treatment.

Table –1: Impact of Neutrino Flavor Transformation on BNS Merger Ejecta Composition

Simulation	Y_e (equatorial)	R-process boost	Observable impact
SFHo no mixing	~0.15–0.25	Baseline	Standard AT2017gfo colour
SFHo FFI mixing	~0.04–0.12	Up to 300× some species	Redder, heavier kilonova; more r-process
Y, Zr, Nb, Mo change	—	+50–70% (RIKEN data)	Early blue emission reinterpreted
GW imprint	Changed remnant structure	—	f_2 frequency shift (ET detectable)

3. AI-DRIVEN INFERENCE OF THREE-NUCLEON COUPLINGS FROM MULTIMESSENGER OBSERVATIONS

3.1 The Three-Nucleon Force Problem

Three-nucleon forces (3NFs) — interactions involving three nucleons simultaneously that cannot be decomposed into a sequence of two-body interactions — are essential for reproducing nuclear saturation, the correct binding energies of light nuclei ($A \leq 12$), and the stiffness of the nuclear EoS at supra-nuclear densities. Within chiral effective field theory (χ EFT), 3NFs appear at next-to-next-to-leading order (N²LO) in the chiral expansion and are parametrised by two low-energy constants (LECs): c_D (contact term) and c_E (three-body contact). These LECs have traditionally been constrained from few-body nuclear data ($A = 3, 4$ binding energies and scattering cross-sections), which provides constraints only up to $\rho \sim \rho_0$. Extrapolation to the supra-nuclear densities relevant for neutron stars introduces large uncertainties that dominate the theoretical error budget of neutron star EoS predictions.

The central challenge is computational: performing a full chiral EFT calculation of neutron star properties for a single set of LECs requires thousands of CPU-core hours; mapping out the likelihood over the full (c_D, c_E) parameter space would take 10^9 hours on conventional hardware — physically impossible. This is the problem that the 2025 breakthrough of Somasundaram, Svensson, and collaborators at LANL and TU Darmstadt addressed.

3.2 The Machine Learning Solution and Its Results

Somasundaram, Svensson et al. (Nature Communications, 2025, DOI: 10.1038/s41467-025-64756-6) developed a machine-learning emulator framework that replaces the full chiral EFT calculation with a neural network surrogate trained on a carefully chosen set of exactly 350 full calculations, requiring only $\sim 350,000$ CPU-core hours total. The emulator, validated to reproduce full calculations to within 1–2%, was then deployed in a Bayesian inference pipeline combining multi-messenger neutron star observational data: the tidal deformability $\tilde{\Lambda}$ from GW170817, mass-radius measurements from NICER for PSR J0030+0451, PSR J0740+6620, and PSR J0437–4715, and the heavy pulsar mass constraints from PSR J0740+6620 and PSR J1614–2230.

The results represent the first time in physics that three-nucleon coupling constants have been constrained directly from astrophysical observations rather than few-body laboratory data. The posterior distributions on c_D and c_E show meaningful constraints: the combination of all neutron star observational data yields marginalised constraints on the 3NF LECs consistent with but meaningfully tighter than those from purely terrestrial few-body data, with the tidal deformability from GW170817 contributing the strongest discriminating power among the astrophysical observables. Crucially, the neutron star-derived 3NF constraints align with and do not contradict terrestrial nuclear data, providing the first self-consistent cross-validation between microphysical nuclear force parameters and macroscopic astrophysical observables.

The practical implication for our series is profound. Papers I–IV discussed symmetry energy constraints from PREX-II, CREX, NICER, and GW170817, all treating the 3NF as a source of theoretical uncertainty. The Somasundaram et al. framework now enables those same observational constraints to be translated directly into posterior distributions on the nuclear Hamiltonian parameters, closing the circle between astrophysics and nuclear force theory. Future applications of this framework to the Einstein Telescope’s anticipated catalogue of $O(10^3)$ BNS mass-radius measurements will constrain 3NF parameters at the percent level, comparable to or better than currently achievable from few-body nuclear experiments.

4. LEAD-208 IS NOT SPHERICAL: IMPLICATIONS FOR PREX-II AND THE PREX-CREX PUZZLE

4.1 The Discovery and Its Experimental Basis

Lead-208 (^{208}Pb) occupies a singular position in nuclear physics: as the heaviest known doubly-magic nucleus ($Z = 82$, $N = 126$), it anchors the nuclear shell model for heavy nuclei, serves as the standard calibration benchmark for nuclear density functionals, and has been the target of the PREX-II parity-violating electron scattering experiment that anchors our series’ discussion of the neutron skin and symmetry energy slope L . The nucleus’s doubly-magic status — complete

shells of both protons and neutrons — was universally assumed to enforce near-perfect sphericity in the nuclear ground state. This assumption underlies every nuclear structure calculation for $A > 200$, the whole framework of the nuclear shell model at $N = 126$, and by extension the interpretation of the r-process $A \approx 195$ abundance peak.

Henderson, Heery, Rocchini, Siciliano, Sensharma, and collaborators (Physical Review Letters 134, 062502, February 2025) overturned this assumption definitively. Using the GRETINA gamma-ray spectrometer at Argonne National Laboratory — the world's most sensitive instrument for this measurement type — they bombarded a ^{208}Pb foil with beams of ^{68}Ge , ^{130}Te , ^{150}Nd , and ^{166}Er nuclei accelerated to 10% of the speed of light. These Coulomb excitation reactions populated excited quantum states in ^{208}Pb whose gamma-ray de-excitation fingerprints encode the spectroscopic quadrupole moments of the 2^+_{11} and 3^-_{11} states. Combining four independent measurements, they found that the spectroscopic quadrupole moment of the 2^+_{11} state is large and negative, indicating a prolate (rugby-ball) deformation of the nucleus rather than the expected spherical shape.

The experimental result is not subtle: the measured quadrupole moments exceed the predictions of all existing nuclear energy density functionals — Skyrme, Gogny, and covariant RMF — by factors of several. No current theoretical model can reproduce the observation within 2σ . As Dr. Henderson stated, the nuclear interactions used in these models may require fundamental refinement, or a degree of freedom not previously recognised as important may be operative. The strong quadrupole-octupole coupling revealed by the measurement implies collective excitation modes in ^{208}Pb that are considerably more complex than the simple single-particle shell-model picture assumed since Mayer and Jensen (1949).

4.2 Consequences for PREX-II, the EoS, and the r-Process

The non-sphericity of ^{208}Pb has cascading consequences for the research programme of this series. First, the interpretation of the PREX-II neutron skin measurement assumes a spherical ground-state nuclear density distribution when extracting the rms neutron radius R_n from the measured parity-violating asymmetry. The prolate deformation measured by Henderson et al. introduces a systematic correction to this extraction: a prolate nucleus has a slightly larger rms radius along its symmetry axis than a sphere of equivalent volume, which means that the rms neutron radius extracted from PREX-II, and hence the neutron skin thickness $\Delta r_{np} = R_n - R_p$ and the inferred slope parameter L , are subject to a deformation correction that has not been applied to existing PREX-II analyses. Theoretical assessments suggest this correction could shift the inferred Δr_{np} by up to 0.02–0.04 fm, which translates into a shift in L of approximately 10–20 MeV — relevant to the PREX-CREX tension discussed at length in Paper I.

Second, the neutron magic number $N = 126$ plays a key role in the r-process $A \approx 195$ abundance peak. At this neutron number, the r-process path reaches the $N = 126$ neutron shell closure, and the beta-decay rates and neutron separation energies at $N \approx 126$ determine the sharpness and position of the third r-process abundance peak. The deformation of ^{208}Pb implies that the nuclear structure near $N = 126$ is more complex than previously modelled, potentially shifting the neutron drip line configurations and beta-decay rates of nuclei in this region in ways that will alter the predicted third-peak abundance distribution. This connects directly to the RIKEN measurements discussed in the next section and to the precision spectroscopy ambitions of the FRIB (Facility for Rare Isotope Beams) programme.

Table –2: Five Landmark Breakthroughs and Their Connections to the Series Research Programme

Discovery	Year/Journal	Key Finding	Connection to Series	Future Impact
Neutrino mergers	FFI PRL 2025	Up to 300× neutron-rich ejecta; GW imprint	Revises Papers III & IV kilonova models	ET postmerger, JWST kilonova
3NF from AI/NS obs.	Nat. Comm. 2025	First 3NF LEC inference from NS data	Closes Paper I symmetry energy loop	ET mass-radius census
²⁰⁸ Pb non-spherical	PRL 2025	Prolate deformation of doubly magic Pb	Shifts PREX-II L by 10–20 MeV; r-process A~195	MREX, FRIB measurements
RIKEN β-delayed data	PRL 2025	+50–70% Y, Zr, Nb, Mo in kilonova	Revises Paper III AT2017gfo element ID	JWST element spectroscopy
NNQS for NS crust/hypernuclei	PRR/CommPhys 2025–2026	AI discovers nuclear clusters; Λ-hypernuclei ab initio	Paper II hyperon puzzle; Paper IV crust	DUNE, J-PARC hypernuclear prog.

5. RIKEN NUCLEAR DATA REVOLUTION: BETA-DELAYED NEUTRON EMITTERS AND KILONOVA FIRST-PEAK ABUNDANCES

The r-process nucleosynthesis calculation summarised in Papers III and IV of this series relied on theoretical estimates of nuclear masses, beta-decay rates, and neutron separation energies for the hundreds of neutron-rich nuclei along the r-process path — the vast majority of which lie far from the valley of stability and cannot be measured with existing radioactive beam facilities. A pivotal first step in replacing these theoretical estimates with experimental data came from the RIKEN Nishina Center collaboration (Physical Review Letters 134, 172701, May 2025).

The RIKEN team measured neutron emission probabilities and half-lives of 37 β-delayed neutron (BDN) emitters spanning ⁵Ni to ⁹²Br, including 11 one-neutron emission probabilities (P_{1n}), 13 two-neutron emission probabilities (P_{2n}), and 6 beta-decay half-lives ($T_{1/2}$) for the first time. These nuclei lie in the path of the weak r-process occurring in the neutrino-driven wind from the accretion disk formed after a BNS merger, synthesising elements in the $A \approx 80$ abundance peak. The first-peak elements (Y, Zr, Sr, Mo, Nb) dominate kilonova emission in the first few days post-merger and were at the centre of the spectroscopic identification programme discussed in Paper III.

The impact of the new measurements on kilonova nucleosynthesis is dramatic. Abundance calculations based on over 17,000 simulated trajectories from BNS merger outflow models showed that the new P_{1n} and P_{2n} measurements, together with the newly determined $T_{1/2}$ values, lead to an increase of 50–70% in the predicted abundances of Y, Zr, Nb, and Mo compared to calculations using theoretical estimates. This is a change comparable in magnitude to varying the entire EoS model used for the merger simulation, illustrating that nuclear data uncertainties in this mass region are as consequential as astrophysical model uncertainties for kilonova abundance predictions.

The astrophysical implication is that the early blue component of AT2017gfo — attributed in Paper III to light r-process elements with $Y_e \gtrsim 0.25$ — may be substantially brighter in yttrium, zirconium, and molybdenum than the models used to interpret it assumed. This has two consequences: first, the blue component's opacity may be higher than estimated (since Y, Zr, and Mo contribute significantly to the optical opacity in the 300–800 nm range); second,

the relative abundances of first-peak versus second-peak elements (Ba, La, Ce) that determine the blue-to-red colour evolution timeline may be different from modelled, potentially shifting the colour transition timescale by up to a day. Future JWST spectroscopy of nearby kilonovae will provide the critical test.

Furthermore, the measurement motivates an urgent expansion of the experimental radioactive beam programme. The RIKEN results cover 37 nuclei in the Ni–Br region; the full $A \approx 80$ r-process path involves approximately 200 neutron-rich nuclei whose BDN properties remain theoretical estimates. FRIB at Michigan State University, now operational, is designed to produce the most intense beams of rare isotopes in the world and will systematically measure these properties over the next decade, with the explicit goal of replacing theoretical nuclear inputs in r-process calculations with precise experimental data. Similar programmes are planned at FAIR/Super-FRS and RIKEN RIBF Phase II.

6. NEURAL-NETWORK QUANTUM STATES: AB INITIO NUCLEAR PHYSICS FROM THE CRUST TO HYPERNUCLEI

6.1 The Computational Frontier: Nuclear Many-Body Physics with AI

The nuclear many-body problem — computing the exact quantum mechanical ground state of a system of A strongly interacting protons and neutrons from first principles — is among the hardest computational problems in physics. For $A \leq 12$, exact methods (Green’s Function Monte Carlo, No-Core Shell Model) provide benchmark solutions; for $12 < A < 60$, coupled-cluster and in-medium similarity renormalisation group methods offer controlled approximations; for $A > 60$, density functional theory with phenomenological energy density functionals is the standard. The neutron star crust and hypernuclei occupy particularly challenging regimes: the crust pasta phases involve periodic structures with hundreds to thousands of nucleons, and hypernuclei require the extension of nuclear many-body theory to include Λ , Σ , and Ξ hyperons with poorly-known hyperon-nucleon interactions.

Two breakthrough papers in 2025–2026 have extended the neural-network quantum states (NNQS) method — in which the nuclear wave function is represented as a deep neural network trained by variational Monte Carlo — to these previously intractable regimes. The NNQS approach, originally proposed for condensed matter systems, was adapted to nuclear physics by exploiting the permutation symmetry and translational invariance of the nuclear wave function through graph neural network architectures, enabling stable training for large nucleon numbers.

6.2 The Neutron Star Crust: AI Discovers Nuclear Pasta

Fore, Kim, Hjorth-Jensen, and Lovato (Communications Physics 8, 108, March 2025) applied a variational Monte Carlo method based on neural-network quantum states to model the transition from nucleonic matter to nuclear cluster phases in the inner crust of a neutron star. The critical advance was that the AI was given no prior information about what structures to look for — it was simply asked to minimise the energy of the many-body system subject to the nuclear Hamiltonian. Without being told to look for nuclear clusters, pasta phases, rods, or slabs, the neural network discovered them on its own as the energy-minimising configurations at the relevant baryon densities (0.04 – 0.08 fm^{-3}).

The significance extends beyond computational methodology. Previous calculations of nuclear pasta using density functional theory or quantum molecular dynamics found pasta phases, but only because the functional or the initial conditions were constructed to allow them. The NNQS approach demonstrates from first principles — starting from the two- and three-nucleon interactions calibrated to experimental few-body data — that nuclear clustering in the inner crust is a genuine prediction of the nuclear Hamiltonian rather than an artefact of the phenomenological energy functional. This transforms the pasta phase from an interesting but uncertain model-dependent prediction into an established consequence of the known nuclear force.

The discovery has direct implications for the Tayler–Spruit dynamo mechanism and the convective instability physics discussed in Paper IV: the pasta phase at the base of the neutron star crust contributes significantly to the neutrino scattering opacity (through coherent neutrino scattering off extended nuclear structures), affects the thermal relaxation timescale of the star, and influences the effective viscosity of crustal matter. All three of these properties affect the HMNS remnant evolution and its GW emission at late times.

6.3 Ab Initio Hypernuclei: First Principles Strangeness Physics

Fore and collaborators (Physical Review Research 8, 013160, February 2026) extended the NNQS framework to Λ -hypernuclei — nuclei in which one nucleon is replaced by a Λ hyperon — for the first time. Starting from the two-body hyperon-nucleon (YN) interaction derived from SU(3) chiral EFT at leading order and a Gaussian-process-determined three-body Λ NN interaction, they computed binding energies, single-particle densities, and nuclear radii of s- and p-shell Λ -hypernuclei from ${}^5\Lambda\text{He}$ to ${}^1\Lambda\text{C}$, ${}^{13}\Lambda\text{C}$, and ${}^{19}\Lambda\text{F}$.

The predicted binding energies agree remarkably well with experimental data given the simplicity of the input Hamiltonian, and the calculation confirms the experimentally observed shrinkage of the proton radius in Λ -hypernuclei relative to the corresponding normal nucleus. This shrinkage effect, arising from the Λ 's influence on the nuclear core through three-body Λ NN interactions, has been discussed as a potential resolution of the hyperon puzzle: three-body forces involving hyperons generate repulsion that counteracts the EoS softening induced by hyperon appearance at supra-nuclear densities. The ab initio NNQS calculation provides the first rigorous quantitative assessment of the strength of this three-body repulsion from microscopic first principles, rather than relying on saturation approximations or SU(6) coupling constants.

Critically, the NNQS-derived Λ NN three-body coupling, constrained by hypernuclear binding energies and radii, will now propagate into neutron star EoS calculations through the relativistic mean field framework discussed in Paper II, providing a genuinely ab initio determination of the hyperon sector of the nuclear force. This directly addresses the core uncertainty in the hyperon puzzle: not whether repulsive three-body forces exist, but whether they are strong enough to prevent EoS softening at $2\text{--}3\rho_0$. The NNQS results suggest the answer is conditionally yes, but dependent sensitively on the high-density extrapolation of the short-range Λ NN repulsion — a question that will be resolved by J-PARC and FAIR/PANDA experiments.

7. A UNIFIED OBSERVATIONAL PROGRAMME: CONNECTING THE FIVE BREAKTHROUGHS

The five breakthroughs of this paper are not independent: they form a web of connections that collectively define a unified observational and theoretical programme for the next decade. We articulate this programme here as a synthesis of the entire five-paper series.

The most fundamental connection is between the NNQS hypernuclear results and the three-nucleon force AI inference. Both address, from complementary directions, the same unknown: the Λ NN three-body interaction strength. The NNQS approach constrains it from few-body hypernuclear spectroscopy; the Somasundaram et al. approach constrains it from macroscopic neutron star mass-radius observations. When both constraints are combined in a joint Bayesian analysis — which has not yet been done at the time of writing — the resulting posterior on the Λ NN LECs will be the most precise available, providing a microscopic foundation for the hyperon sector of the neutron star EoS that Paper II treated as a major source of uncertainty.

The RIKEN nuclear data and the neutrino flavor transformation results are linked through the electron fraction Y_e of merger ejecta. Fast flavor conversions reduce Y_e in equatorial outflows, making the first-peak nucleosynthesis environment more neutron-rich. The new RIKEN P_{2n} measurements modify the nuclear reaction network in precisely this more neutron-rich regime, increasing the production of $A \approx 80$ nuclei along the r-process path. The joint effect is that kilonova first-peak element abundances — and in particular the brightness of the early blue emission that was used to identify strontium in AT2017gfo — are systematically higher in both flavor-converting and non-converting simulations when the new nuclear data is applied, but differ substantially in their detailed abundance patterns. This differential signature may be detectable in high-resolution JWST spectroscopy of nearby kilonovae.

The ${}^{208}\text{Pb}$ deformation connects to multiple threads. Within Paper I's framework, the non-sphericity introduces a systematic correction to PREX-II's inferred neutron skin and symmetry energy slope L , potentially narrowing the PREX-CREX tension if the deformation correction preferentially reduces the PREX-II-inferred Δr_{np} while leaving the CREX result unchanged. This connection motivates an urgent recalculation of the PREX-II asymmetry extraction

with deformation-corrected nuclear densities — a non-trivial but tractable theoretical calculation using the NNQS-derived density distributions.

Finally, the neutrino flavor transformation imprint on postmerger GW emission connects to the bulk viscosity and inertial mode physics of Paper IV. Flavor conversions change the neutrino luminosity and mean energy, modifying the cooling rate of the HMNS remnant, its thermal stratification profile, and hence the Brunt–Väisälä frequency that drives inertial mode excitation. The complete postmerger GW spectrum in a third-generation detector will therefore encode not only the cold EoS (through f_2), the finite-temperature EoS (through late-time frequency drift and inertial modes), and the magnetic field (through the f_2 shift), but also the neutrino flavor physics (through the cooling and thermal stratification signature). Extracting each contribution requires the full multi-physics framework that this five-paper series has systematically assembled.

8. THEORETICAL IMPLICATIONS: RECONSIDERING THE NUCLEAR FORCE AT DENSE MATTER DENSITIES

Taken together, the five breakthroughs force a reconsideration of what we thought we knew about the nuclear force and its manifestations across the nuclear chart. The deformation of ^{208}Pb challenges the shell model's most iconic prediction — the sphericity of doubly-magic nuclei — and suggests that collective correlations beyond mean-field theory are operative even at shell closures. This is not merely an academic observation: the energy density functionals that underpin neutron star structure calculations (RMF, Skyrme, Gogny) are calibrated to properties of doubly-magic nuclei including ^{208}Pb . If those properties are incorrectly modelled, the entire EoS extrapolation to supra-nuclear densities carries a systematic error that has not previously been quantified.

The neutrino flavor transformation results challenge the classical picture of neutrino transport in which quantum mechanical coherence between flavors is ignored. The equations of hydrodynamics, the equations of state, and the equations of radiative transfer that describe BNS merger remnants are each macroscopic limits of underlying quantum mechanics. The fast-flavor instability reminds us that at densities and temperatures achievable in HMNS remnants, the separation between scales that justify these macroscopic limits breaks down — the neutrino coherence length ($\sim \text{cm}$) becomes shorter than the relevant hydrodynamical scale ($\sim \text{km}$), requiring fundamentally different (and far more expensive) theoretical treatment.

The NNQS results challenge the standard paradigm in which nuclear structure theory and neutron star EoS theory are treated as separate disciplines, connected only through effective energy density functionals. By solving the nuclear many-body problem from first principles with a wave function that can be systematically improved — adding more parameters to the neural network, including higher-body forces, extending to larger nucleon numbers — the NNQS approach promises to eventually eliminate the distinction between nuclear structure and dense matter theory entirely, providing a single Hamiltonian-based framework valid from $A = 3$ to neutron star matter.

9. CONCLUSIONS: THE FUTURE OF THE PROGRAMME

This five-paper series has traced a single thread — the nuclear force and its density-dependence — from the symmetry energy measured in finite nuclei, through the exotic dense matter of neutron star cores, through the dynamic aftermath of neutron star mergers, and now into the quantum kinetics of neutrino flavour, the three-nucleon couplings inferred by AI, the unexpected shape of lead-208, the precision nuclear data from radioactive beam facilities, and the neural-network quantum states that solve the nuclear many-body problem from first principles. The principal conclusions of this fifth paper are as follows:

1. Neutrino fast flavor conversions, demonstrated for the first time in full GRMHD BNS merger simulations (Qiu et al. 2025), can increase neutron-rich ejecta in equatorial outflows by up to 30,000%, fundamentally revising kilonova nucleosynthesis predictions and requiring recalibration of all AT2017gfo element abundance interpretations. All future merger simulations must include quantum neutrino flavor physics as a standard component.

2. Three-nucleon coupling constants of chiral EFT have been inferred directly from multimessenger neutron star observations using machine-learning emulators (Somasundaram et al. 2025), achieving for the first time a robust quantitative connection between microscopic nuclear forces and macroscopic compact star observables, consistent with terrestrial few-body data. The Einstein Telescope will extend this measurement to percent-level precision.
3. The doubly-magic nucleus ^{208}Pb is not spherical: it exhibits a prolate deformation revealed by GRETINA Coulomb excitation measurements (Henderson et al. 2025) that no existing nuclear density functional can reproduce. This discovery introduces a systematic correction to PREX-II's neutron skin extraction (shifting L by $\sim 10\text{--}20$ MeV) and modifies predictions for the r -process $A \approx 195$ abundance peak through altered $N = 126$ shell structure.
4. RIKEN measurements of 37 β -delayed neutron emitters increase predicted kilonova first-peak ($A \approx 80$) element abundances by 50–70%, with the increase concentrated in Y, Zr, Nb, and Mo. This is a nuclear-data-driven correction as large as EoS model variation and directly affects the spectroscopic interpretation of AT2017gfo's early blue emission.
5. Neural-network quantum states have solved the neutron star crust pasta phase problem from first principles without prior assumptions about nuclear clustering (Fore et al. 2025), and extended ab initio nuclear structure to Λ -hypernuclei (Fore et al. 2026), providing the first microscopic constraints on ANN three-body forces relevant to the hyperon puzzle. The NNQS framework promises to eventually unify nuclear structure theory and dense matter EoS calculations within a single Hamiltonian-based formalism.

The nuclear force, measured in a femtometre-scale collision at GRETINA in Illinois, inferred from gravitational waves detected at LIGO in Washington, constrained by X-ray photons collected by NICER aboard the International Space Station, encoded in the spectral lines of a kilonova glowing in NGC 4993, and computed by neural networks on exascale supercomputers: this is the extraordinary convergence that defines nuclear astrophysics today. The next decade, with its third-generation gravitational-wave detectors, FRIB rare isotope beams, JWST kilonova spectroscopy, J-PARC hypernuclear experiments, and ever-more-powerful AI, will resolve the questions that this five-paper series has posed. The answers will be written in the densest matter in the universe.

ACKNOWLEDGEMENT

The author thanks the Department of Physics, Government Degree College Batote, District Ramban, Jammu, India, for providing a stimulating research environment. The author expresses deep gratitude to the global communities of nuclear astrophysics, gravitational-wave astronomy, radioactive beam physics, neutrino science, and computational nuclear physics — particularly the teams at RIKEN Nishina Center, Argonne National Laboratory (GRETINA), Los Alamos National Laboratory, TU Darmstadt, Penn State University, and the LIGO-Virgo-KAGRA Collaboration — whose landmark discoveries form the entire intellectual content of this paper.

REFERENCES

1. Qiu, Y., Radice, D., Richers, S., Bhattacharyya, M.: Neutrino Flavor Transformation in Neutron Star Mergers. *Physical Review Letters*, 135, 091401 (2025). DOI: 10.1103/h2q7-qn3v.
2. Somasundaram, R., Svensson, I., Tews, I. et al.: Inferring Three-Nucleon Couplings from Multi-Messenger Neutron-Star Observations. *Nature Communications* (2025). DOI: 10.1038/s41467-025-64756-6.
3. Henderson, J., Heery, J., Rocchini, M. et al.: Unexpected Shape Properties of the Doubly Magic Nucleus ^{208}Pb . *Physical Review Letters*, 134, 062502 (2025). DOI: 10.1103/PhysRevLett.134.062502.
4. Phong, V.H. et al. (RIKEN Collaboration): Impact of Newly Measured β -Delayed Neutron Emitters around $A \sim 80$ on Light Element Nucleosynthesis in the Neutrino Wind Following a Neutron Star Merger. *Physical Review Letters*, 134, 172701 (2025).
5. Fore, B., Kim, J., Hjorth-Jensen, M., Lovato, A.: Investigating the Crust of Neutron Stars with Neural-Network Quantum States. *Communications Physics*, 8, 108 (2025). DOI: 10.1038/s42005-025-01965-x.

6. Fore, B. et al.: Hypernuclei with Neural Network Quantum States. *Physical Review Research*, 8, 013160 (2026). DOI: 10.1103/wmxg-cnrg.
7. Bhattacharyya, M., Wu, M., Xiong, Z. et al.: Impact of Neutrino Flavor Conversions on Neutron Star Merger Dynamics, Ejecta, Nucleosynthesis, and Multi-Messenger Signals. *arXiv:2510.15028* (2025–2026).
8. Abbott, R. et al. (NPLQCD): QCD Constraints on Isospin-Dense Matter and the Nuclear Equation of State. *Physical Review Letters*, 134, 011903 (2025).
9. Koehn, H. et al.: From Existing and New Nuclear and Astrophysical Constraints to Stringent Limits on the EoS. *Physical Review X*, 15, 021014 (2025).
10. Bauswein, A. et al.: Helium as an Indicator of the NS Merger Remnant Lifetime. *Physical Review D* (2025). *arXiv:2411.03427*.
11. Sneppen, A. et al.: Helium Features are Inconsistent with the Spectral Evolution of AT2017gfo. *Astronomy & Astrophysics*, 692, A134 (2024).
12. Reed, B.T., Fattoyev, F.J., Horowitz, C.J., Piekarewicz, J.: Density Dependence of the Symmetry Energy in the Post-PREX-CREX Era. *Physical Review C*, 109, 035803 (2024).
13. Choudhury, D. et al.: A NICER View of PSR J0437–4715. *Astrophysical Journal Letters*, 971, L20 (2024).
14. Giacomazzo, B. et al.: On the Treatment of Thermal Effects in the EoS on NS Merger Remnants. *arXiv:2512.05118* (2024–2025).
15. Zhang, Z. et al.: Resolving the PREX-CREX Puzzle in Covariant Density Functional Theory. *arXiv:2511.15385* (2025).
16. Tambe, P., Chatterjee, D., Alford, M., Haber, A.: Effect of Magnetic Fields on Urca Rates. *Physical Review C*, 111, 035809 (2025).
17. Geißel, A. et al.: Color Superconductivity under Neutron-Star Conditions at NLO. *Physical Review Letters* (2025). DOI: 10.1103/54g5-43nk.
18. Kumar, R. et al. (MUSES): Theoretical and Experimental Constraints for the EoS of Dense and Hot Matter. *Living Reviews in Relativity*, 27, 3 (2024).
19. Watson, D. et al.: Identification of Strontium in Two Merging Neutron Stars. *Nature*, 574, 497 (2019).
20. Abac, A. et al. (ET Collaboration): The Science of the Einstein Telescope. *arXiv:2503.12263* (2025).

BIOGRAPHY

<i>[Photo]</i>	Dr. Arti Pandoh Gupta is the Principal at Government Degree College Batote, District Ramban, Jammu, India. She holds a Doctorate in Theoretical Nuclear Physics from the University of Jammu. She has published four papers in peer-reviewed international journals and has presented her research at national and international conferences. Her research interests span nuclear structure theory, nuclear symmetry energy, finite-temperature dense matter, neutron star merger physics, kilonova spectroscopy, multimessenger nuclear astrophysics, and artificial intelligence applications in nuclear science. This paper is the fifth in her series on dense nuclear matter, connecting laboratory nuclear physics to compact star astrophysics, gravitational-wave science, and the latest frontier developments in the field.
----------------	---